Comparison between Delay and Sum and Range Migration Algorithms for Image Reconstruction in Through-the-Wall Radar Imaging Systems

S. Pisa, *Senior Member, IEEE*, E. Piuzzi, *Member, IEEE*, E. Pittella, *Member*, *IEEE,*
P. D'Atanasio, A. Zambotti, G. Sacco, *Student Member*, *IEEE*

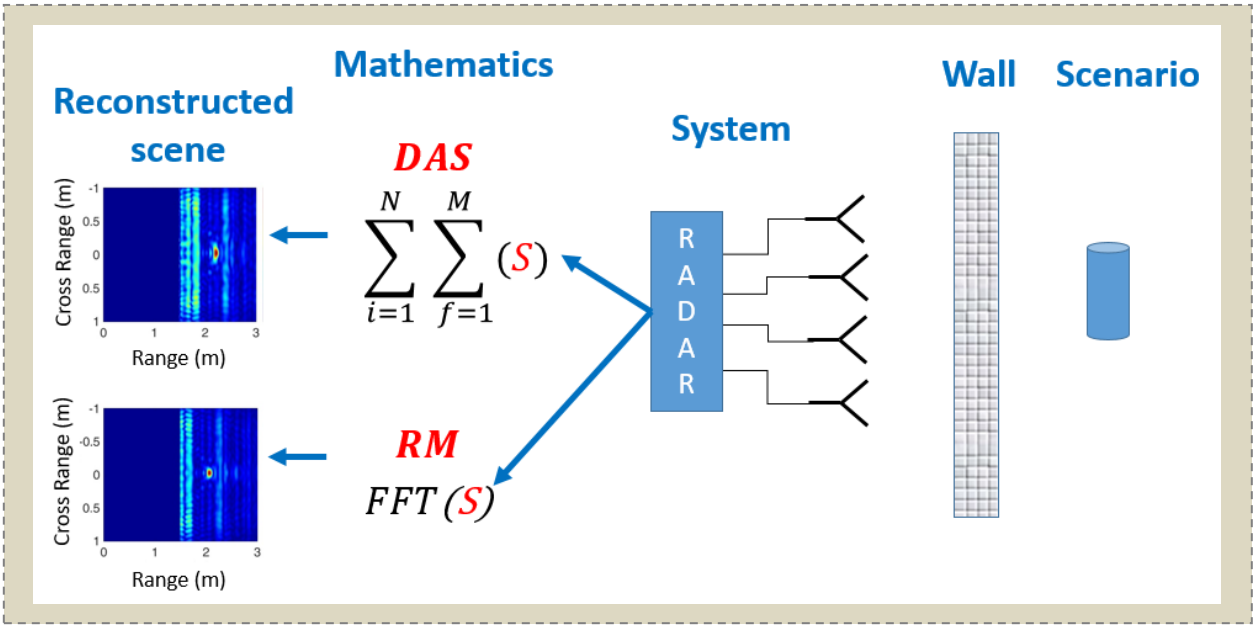

Two reconstruction algorithms operating on scattering parameters measured by a stepped-frequency radar are compared in terms of accuracy and speed of through-the-wall image reconstruction

Take-Home Messages

- TWRI systems can remotely monitor thieves or robbers inside a building or subjects under the rubble.
- Delay and sum (DAS) and range migration (RM) algorithms are among the most used techniques for image reconstruction and in this paper their pros and cons are investigated.
- The two inversion algorithms have been compared based on analytical, numerical and experimental data acquired for realistic scenarios.
- DAS and RM have similar resolution and dynamics with the former having a better field of view and the latter being faster.

Comparison between Delay and Sum and Range Migration Algorithms for Image Reconstruction in Through-the-Wall Radar Imaging Systems

S. Pisa, *Senior Member, IEEE*, E. Piuzzi, *Member, IEEE*, E. Pittella, *Member*, *IEEE,*
P. D'Atanasio, A. Zambotti, G. Sacco, *Student Member*, *IEEE*

Abstract Through-the-wall radar imaging (TWRI) systems allow police, fire personnel and defense forces to detect, identify and track subjects inside buildings or under rubble. In this paper, the delay and sum (DAS) and range migration (RM) algorithms are compared as imaging techniques for a multiple input multiple output (MIMO) stepped-frequency (SF) radar system. These algorithms have been applied to analytical, simulated, and measured data both in the absence and in the presence of a wall between the antenna and the target. Both techniques were able to accurately reconstruct the position of targets behind a wall. The DAS presents a wider angle of non-ambiguity while the RM is faster. An improvement of the DAS, in terms of accuracy in the target positioning, is achieved applying the Fermat's principle.

Keywords **— Delay and Sum algorithm, Fermat's principle, Range Migration algorithm, Through-the-wall radar imaging**

I. Introduction

Through-the-wall radar imaging (TWRI) systems allow police, fire personnel and defense forces to detect, identify and track subjects inside buildings [1]. Moreover, they can also be used to track elderly adults inside their home in the active and assisted living (AAL) context [2]. Generally, these systems utilize a time-division multiplexed (TDM) multiple-input multiple-output (MIMO) array of antennas and are based on frequency modulated continuous wave (FMCW) [3]-[5], ultra-wideband (UWB) [6] or stepped-frequency (SF) radars [7]-[10]. TWRI systems apply algorithms on the acquired signals in order to reconstruct an image of the investigated scenario. Lincoln-MIT laboratory used, as imaging technique, the range migration (RM) algorithm [3], [4] applied to FMCW radar data; while, at the Army Research Laboratory, the back projection (delay and sum (DAS)) time domain algorithm has been implemented [6]. Finally, The Villanova University group developed a compressive sensing technique applied to the output signals of a stepped-frequency radar [7]-[8].

In this paper, a stepped-frequency radar will be considered and the frequency domain delay and sum and range migration algorithms will be utilized for the image reconstruction.

In particular, DAS and RM will be applied to scattering parameters analytically evaluated for a single point scatterer and for a cylinder behind a wall (2D-problem). Moreover, the two algorithms will be implemented on simulated scattering parameters achieved with a full-wave electromagnetic CAD (Microwave Studio by CST) simulating a cylindrical obstacle behind a wall. Finally, an experimental setup constituted by a dielectric and two scatterers behind a brick wall will be considered. In this case, the scattering parameters measured with a vector network analyzer (VNA) at the port of two truncated waveguide antennas will be given as input to the DAS and RM algorithms. By using analytical, simulated and measured data, the potentiality and limits of the DAS and RM techniques will be deeply investigated.

This work was supported in part by the Italian Ministry of University and Research under the PRIN 2015: U-VIEW (Ultra-wideband Virtual Imaging Extra Wall for high-penetration high quality imagery of enclosed structures). S. Pisa, E. Piuzzi, E. Pittella, G. Sacco are with the Department of Information Engineering, Electronics and Telecommunication of Sapienza University of Rome, Via Eudossiana, 18, 00184 Rome, Italy (e-mail: stefano.pisa@uniroma1.it, emanuele.piuzzi@uniroma1.it, erika.pittella@uniroma1.it, giulia.sacco@uniroma1.it). P. D'Atanasio, A. Zambotti are with Italian National Agency for New Technologies, Energy and Sustainable Economic Development, Casaccia Research Centre, Rome 00123, Italy (e-mail: paolo.datanasio@enea.it, alessandro.zambotti@enea.it).

II. Materials and Methods

A. Radar System and Scenarios

Fig. 1 shows the stepped-frequency radar structure. The system utilizes a vector network analyzer that measures the S_{21} scattering parameter between a transmitting and a receiving section. A power amplifier (PA) in the transmitting channel and a low-noise amplifier (LNA) in the receiving one are used to achieve the required dynamics. A couple of switches select sequentially a transmitting and a receiving antenna. The spatial positioning of the transmitting and receiving antennas is chosen to realize a series of equidistant equivalent antennas separated by half the wavelength.

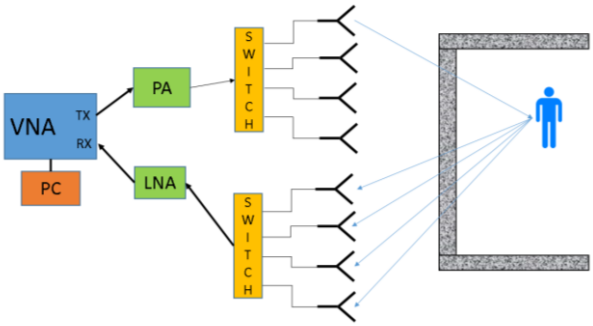

Fig. 1 Stepped-frequency radar structure.

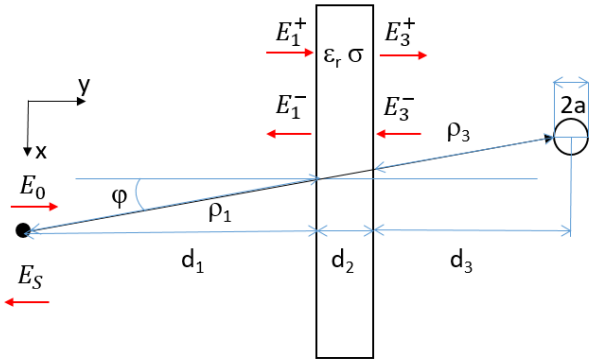

Fig. 2 Analytical geometry.

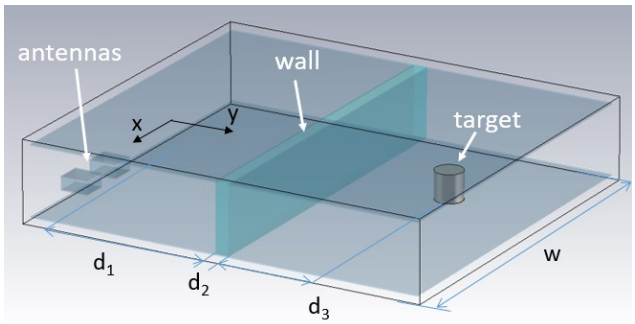

Fig. 3 Simulated scenario.

To test the DAS and RM algorithms, a scenario constituted by M equidistant antennas, a wall and one or two scatterers behind the wall has been considered. For this scenario the SF radar output scattering parameters have been obtained with analytical, simulated and measured approaches.

The analytically studied geometry, depicted in Fig. 2, models one of the radar system equivalent antennas. The transmission line approach has been used to evaluate the scattering parameters. In particular, in the region 1 ($0 < y < d_1$) the following equations hold:

$$E_1^+ = E_0 e^{-jk_0\rho_1} \quad (1)$$

$$E_s = E_1^- e^{-jk_0\rho_1} \quad (2)$$

where:

$$k_0 = \frac{2\pi}{\lambda}. \quad (3)$$

For oblique incidence the air wave impedance in region 1 is given by:

$$Z_1 = \frac{\eta_0}{\cos(\varphi)} \quad (4)$$

where:

$$\eta_0 = \sqrt{\frac{\mu_0}{\varepsilon_0}}. \quad (5)$$

In region 2 ($d_1 \le y \le d_1+d_2$) the wave matrix representation gives:

$$\begin{bmatrix} E_1^+ \\ E_1^- \end{bmatrix} = \frac{1}{T_1 T_2}\begin{bmatrix} e^{j\theta} & R_1 e^{-j\theta} \\ R_1 e^{j\theta} & e^{-j\theta} \end{bmatrix}\begin{bmatrix} 1 & R_2 \\ R_2 & 1 \end{bmatrix}\begin{bmatrix} E_3^+ \\ E_3^- \end{bmatrix} \quad (6)$$

where the normalized wall wave impedance is given by:

$$Z = \frac{Z_2}{Z_1} = \frac{\cos(\varphi)}{\sqrt{(\epsilon_r + \frac{\sigma}{j\omega\epsilon_0}) - \sin^2(\varphi)}} \quad (7)$$

$$R_1 = \frac{Z-1}{Z+1}, \quad R_2 = \frac{1-Z}{Z+1}, \quad T_1 = 1 + R_1, \quad T_2 = 1 + R_2 \quad (8)$$

$$\theta = k_0 d_2 \sqrt{\left(\varepsilon_r + \frac{\sigma}{j\omega\varepsilon_0}\right) - sin^2\varphi}\,. \quad (9)$$

In region 3 ($y > d_1 + d_2$), on the basis of the theory of scattering by a 2D-cylinder, it results [11]:

$$E_3^- = E_3^+ e^{-jk_0\rho_3} \sum_{n=0}^{\infty} (-j)^n \varepsilon_n \frac{J_n(k_0 a)}{H_n^{(2)}(k_0 a)} H_n^{(2)}(k_0\rho_3) \cos n\varphi$$

$$\varepsilon_n = \begin{cases} 1 \text{ for } n = 0 \\ 2 \text{ for } n \neq 0 \end{cases} \quad (10)$$

where J_n and $H_n^{(2)}$ are the Bessel functions of the first kind and the Hankel functions of the second kind, respectively. By solving the system (1)-(10) the E_s field is computed at N frequency points and the scattering parameters can be computed as:

$$S_{11}(\omega) = \frac{E_s(\omega)}{E_0}. \quad (11)$$

The same problem is solved by placing the source at M=27 different positions along the x axis in Fig. 2. The sources are separated by a distance of 7.5 cm (λ/2 at the center frequency of 2 GHz).

In order to investigate the properties of the DAS and RM algorithms, a preliminary study has been performed in the absence of the wall and considering a point scatterer. In this case, the transmission line approach gives:

$$E_s = E_0 e^{-j2k_0\rho_1}. \quad (12)$$

Concerning the numerical and experimental scenario, each equivalent antenna of the radar has been realised with a couple of transmitting and receiving antennas. For the numerical solution, the electromagnetic CAD Microwave Studio by CST has been used (see Fig. 3). To generate the whole set of data, two truncated waveguide antennas, operating in the 1-3 GHz band, with their centers at a

distance of 36 cm, are moved in the cross range direction by 7.5 cm steps at M=27 positions along the x axis. A wall with a thickness d_2 is placed at a distance d_1 from the antennas and a cylindrical metallic target with radius "a" is located at a distance $d_1+d_2+d_3$ from the array. Microwave Studio simulations outputs are the S_{21} scattering parameters between the two antennas at N frequency points.

B. Reconstruction techniques

The first implemented reconstruction technique is the delay and sum algorithm [12]-[13]. In this technique, the domain under study is divided in square pixels (i.e. 1 cm × 1 cm) with (x,y) coordinates and the pixel intensity is evaluated as:

$$I(x,y) = \left| \sum_{k=1}^{M} \sum_{l=1}^{N} \boldsymbol{S}_{\mathbf{ij}}(l) e^{j\frac{2\pi}{\lambda} d(k)} e^{j2\pi f \tau_D} \right| \qquad (13)$$

where i = 1 and j = 1 in the analytical case, while i = 2 and j = 1 in the simulated and measured ones, $d(k)$ is the transmitting antenna–pixel–receiving antenna distance, M is the number of antennas, N the number of considered frequencies, and τ_D is the time delay between the excitation ports and the reference ones. This last term has to be considered only for the simulated and measured scenarios.

For taking into account the refraction caused by the wall, the Fermat's principle of least time [1] has been implemented. Based on this principle, the electromagnetic path between the source and the scatterer and vice versa is the path of least time. This means that the problem of finding $d(k)$ in (13) becomes the optimisation problem of finding the coordinates of points on the wall where the ray meets the wall surfaces for the minimum travel time. This problem has been solved by using the "fminsearch" function of MATLAB® program that implements the multidimensional unconstrained nonlinear minimization (Nelder-Mead) method [14].

The second considered reconstruction technique is the range migration [15]-[16]. In this technique, the scattering parameters at M antenna positions, each one with N frequency points, are allocated in a $S(M\times N)$ matrix.

First, FFT is applied for all columns (along the cross range) with a 256 point zero padding giving:

$$H(k_x, k_r) = \Im\big(S(x,f)\big) \qquad (14)$$

where

$$\frac{-\pi}{d_a} < k_x < \frac{\pi}{d_a}, \qquad (15)$$

d_a is the distance between the antennas and:

$$k_r = \frac{2\pi f}{c} \text{ with } 1\text{ GHz} < f < 3\text{ GHz}. \qquad (16)$$

Then, from the cross range k_x wave number and the range k_r wave number, the k_y wave number is evaluated as:

$$k_y = \sqrt{k_r^2 - k_x^2}. \qquad (17)$$

Introducing an evenly spaced y wave number k_{ye}, the $H(k_x, k_y)$ matrix is interpolated obtaining $H'(k_x, k_{ye})$.

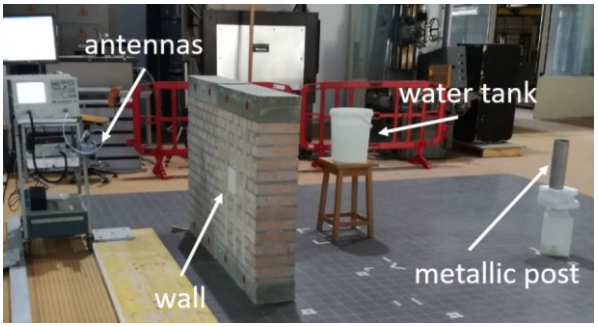

Fig. 4 Experimental setup.

Finally, a 2D inverse FFT is applied giving:

$$I(x,y) = \Im(H'(k_x, k_{ye})) \qquad (18)$$

where $I(x,y)$ represents the reconstructed spatial image.

III. Experiment and Results

A. Experimental Setup

A picture of the experimental setup is reported in Fig. 4. It is constituted by a 25-cm thick brick wall, 180 cm wide, placed at a distance of 80 cm from the antenna aperture plane. A water tank and a metallic post are placed 200 cm and 320 cm from the antenna plane, respectively. The stepped-frequency radar utilizes, as radiating elements, two truncated waveguides (WR 430) operating between 1.7 and 2.6 GHz. The two waveguides, whose centers are at a distance of 46 cm, are moved at 7.5 cm steps at M=31 positions and the S_{21} scattering parameters between the two antennas are measured at N frequency points with a VNA (Agilent PNA-L 5230A). For each antenna position, the measured scattering parameters are stored in the VNA memory and then transferred to a PC for the application of the Matlab codes for the inversion algorithms. In the following, results will be described with reference to analytical, simulated and measured data.

B. DAS and RM with analytical data

The DAS and RM algorithms have been used to reconstruct the scenario from scattering parameters evaluated analytically at N=500 frequency points. First a scenario without the wall has been investigated. For the considered bandwidth (B = 2 GHz) and antenna number (M = 27) placed at distance $d_a = \lambda/2$, the radar theoretical resolution in range is $\delta r = c/2B$ = 7.5 cm and the resolution in angle is $\delta\varphi$ = 1/(M-1) = 0.04 rad. Fig. 5a shows a reconstruction achieved by applying the DAS algorithm to a point scatterer placed at the position x = 0 m, y = 2 m. From image cuts it results a 3 dB width of 7 cm in range (Fig. 6a) and 7 cm in cross-range (Fig. 6b) very close to the 7.5 and 8 cm theoretical values. The same scenario has been reconstructed by using the RM algorithm. The obtained results (not shown) are very similar to those from DAS.

A further study has been performed by moving the target laterally in the x = 2 m, y = 2 m position (φ = 45° in Fig. 2).

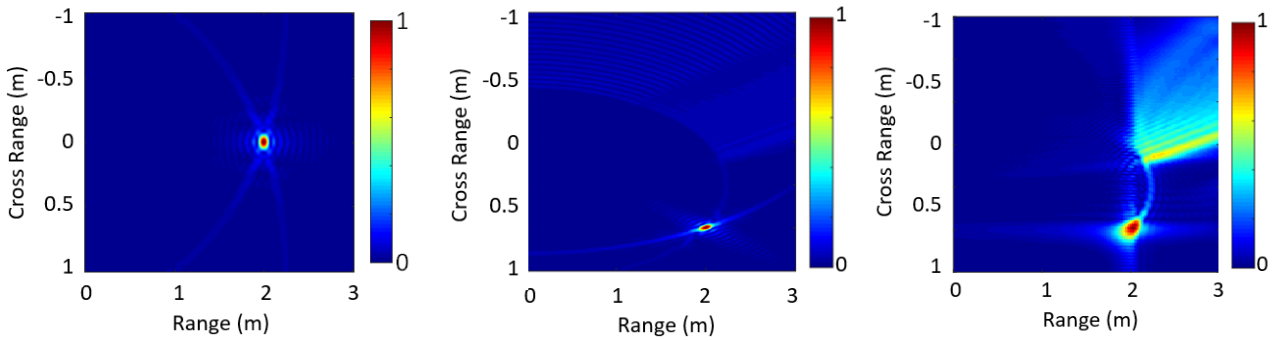

(a) (b) (c)

Fig. 5 Reconstructed images by using DAS and RM on analytical data. Point source with DAS (a), point source with a 45 ° tilt with DAS (b) and with RM (c).

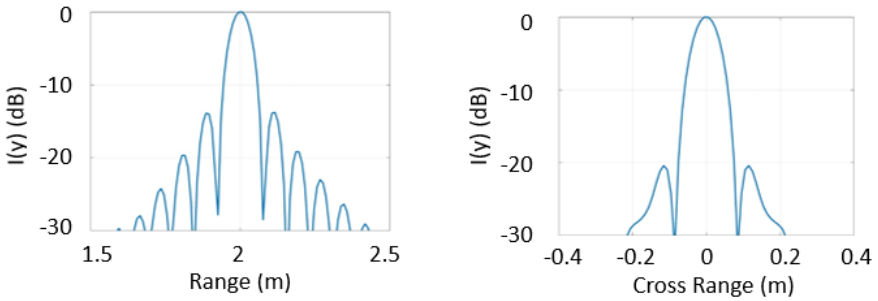

(a) (b)

Fig. 6 Cuts over DAS image of a point source: along range (a) and along cross range (b).

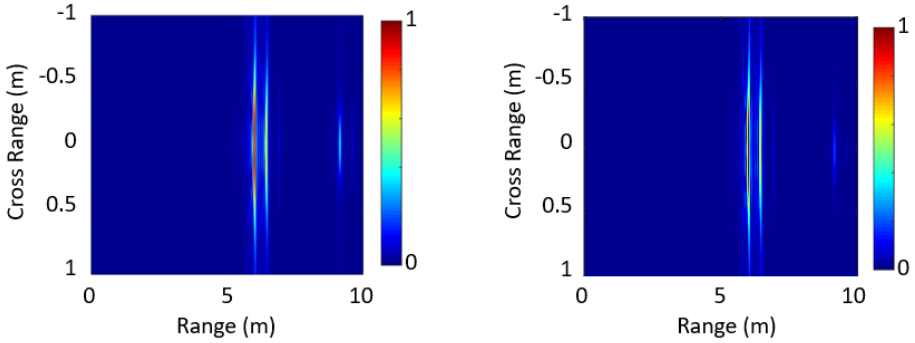

(a) (b)

Fig. 7 Reconstructed images by using DAS and RM on analytical data. Cylinder behind a wall with DAS (a) and with RM (b).

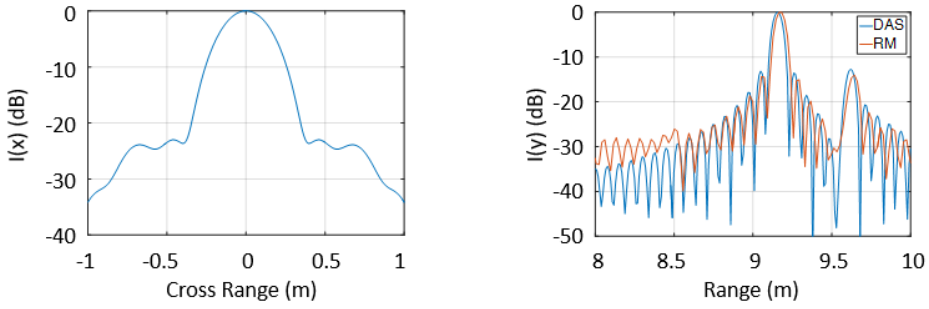

(a) (b)

Fig. 8 Cross range cut over DAS image of a cylinder behind a wall (a) and range cut over DAS and RM images of a cylinder behind a wall (b).

In this case the DAS algorithm is still able to correctly reconstruct the scenario (Fig. 5b) while RM image (Fig. 5c) presents a strong artefact. This is a well known problem of this kind of algorithms that are able to reconstruct the scenario only inside a non-ambiguity angle depending on the antenna spacing. For a half-wavelength spacing the non-ambiguity angle is about 30° and hence lower than the 45° angular direction of the point scatterer investigated.

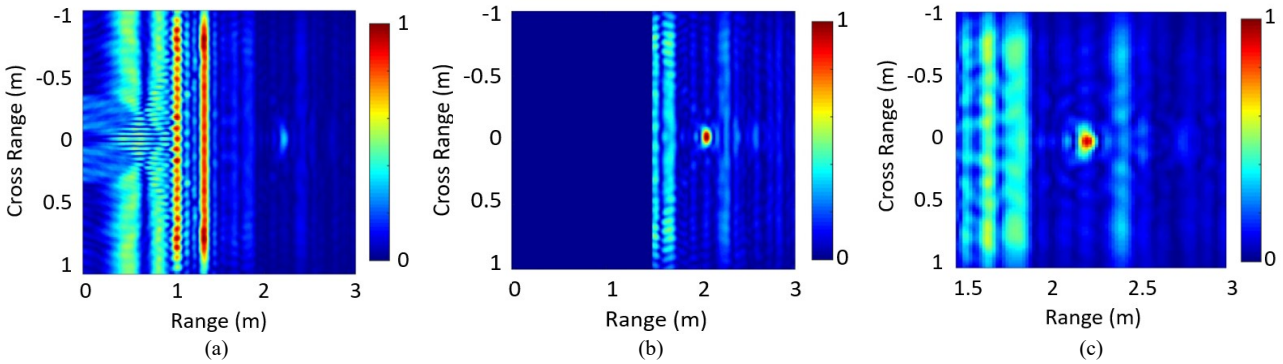

Fig. 9 Reconstructed images from simulated data. DAS reconstruction of a cylinder behind a wall (a); image with DAS and with the application of the Fermat's principle (b); reconstructed image with RM (c).

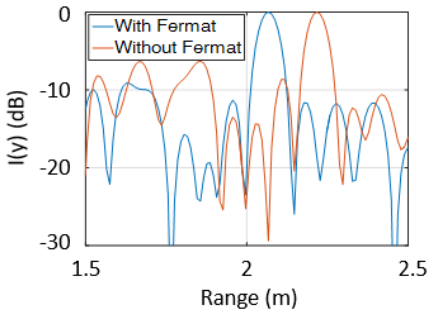

Fig.10 Along range cut of DAS with and without the application of the Fermat's principle.

This problem is not present with the DAS algorithm that hence, from this point of view, has superior performances. A drawback of the DAS is the elaboration time that is longer with respect to the RM. As an example, the solution in Fig. 5a for a 2 m × 3 m domain and 1 cm ×1 cm resolution is achieved in 132 s, with respect to the 2.4 s of RM. However, if the cell dimension is increased to 5 cm × 5 cm the DAS execution time reduces to 5.2 s with still a good localization of the target. Moreover, execution times reduce to 3.7 s by considering 300 frequency points instead of 500.

Finally, Eqs. (1)-(11) have been used to achieve analytically the S_{11} data for the scenario in Fig. 2. In this case d_1 = 6 m, d_2 = 0.2 m, d_3 = 2.8 m, a = 0.1 m, ε_r = 5 and σ = 0.01 S/m. Fig. 7a and Fig. 7b show the DAS and RM images, respectively. The two reconstructions are very similar with a good definition of the two reflecting surfaces of the wall and of the obstacle. Being the obstacle at a distance of 9 m the angular resolution of 0.04 rad gives rise to a theoretical cross range resolution of 36 cm, very close to the 3 dB value of 31 cm obtained from the reconstruction (see Fig. 8a). To further compare the two algorithms, cuts along range on Fig. 7a and Fig. 7b have been overlapped in Fig. 8b. The figure shows that the two techniques have similar range resolution (≈ 7 cm), in agreement with the theoretical one. In addition, dynamic ranges, which are defined as the difference between the peak value and the noise floor, are very similar (≈ 30 dB).

C. *DAS and RM with simulated data*

The simulated scenario consists of a wall with a thickness d_2 = 15 cm, ε_r = 4 and σ = 0 S/m placed at a distance d_1 = 1 m from the antennas and a cylindrical metallic target of radius a = 0.1 m placed 200 cm far from the array. For taking into account the electrical distance between the waveguide excitation plane and the antenna reference plane, a calibration procedure has been applied. In particular, the transmitting and receiving antennas have been placed one in front of the other at various distances and the delay of the transmitted pulse was plotted as a function of the antenna distance. In this manner, the extrapolated delay at a distance equal to zero divided by two gives τ_D. A value of τ_D = 1.5 ns has been estimated for the considered antennas and inserted in (13). By applying the DAS algorithm, the scenario reconstruction of Fig. 9a has been obtained. The strong reflection of the wall is well evidenced, together with the shape of the cylindrical target behind the wall. Then, the Fermat's principle has been applied and the achieved results are reported in Fig. 9b. The figure shows that considering refraction allows a better definition of the target shape and location. In order to better evidence the improvement achieved with the application of the Fermat's principle the along range cut of the images is reported in Fig. 10. The array-cylinder distance of 2 m is estimated as 2.22 m and 2.07 m without and with the application of the Fermat's principle, respectively. By using the RM algorithm the image reported in Fig. 9c has been obtained. The figure shows that the reconstructed array-cylinder distance is about 2.2 m similarly to the DAS without application of the Fermat's principle.

D. *DAS and RM with measured data*

With reference to the measured scenario, this is constituted by a water tank, and a metallic post placed behind a 25 cm thick brick wall located 80 cm far from the antenna (Fig. 4). The antennas are located on a trolley and moved at M = 31 positions. At each position the S_{21} scattering parameters between the two antennas are measured at N=801 frequency points with a VNA (Agilent PNA-L 5230A). A time gating on the measured data has been applied in order to remove the effect of the wall.

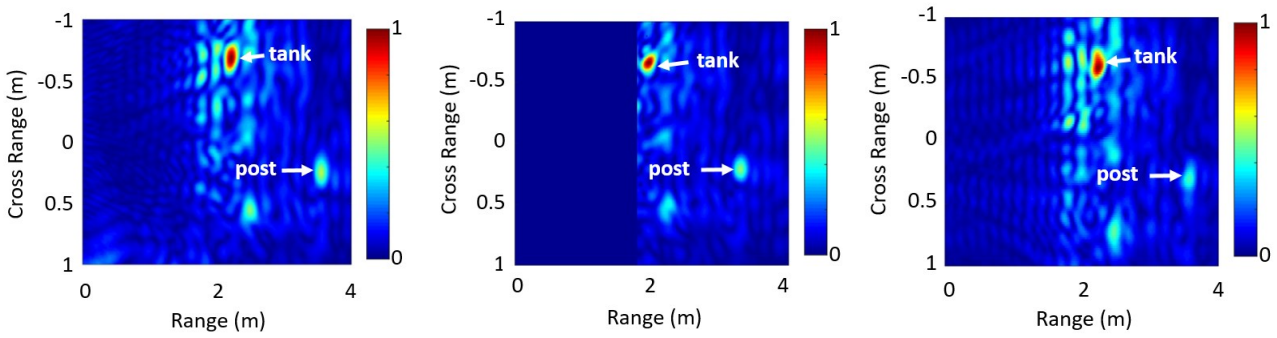

(a) (b) (c)

Fig 11 Reconstructed images from measured data. Two targets behind a wall with DAS (a), DAS with the application of the Fermat's principle (b); image with RM (c).

The achieved reconstructions with the DAS algorithm are reported in Fig. 11a and Fig. 11b, with and without the application of the Fermat's principle. The application of the Fermat's principle gives rise to an improvement in the obstacle shape reconstruction. Fig. 11c shows the image obtained with the RM algorithm. The comparison between Fig. 11a and Fig. 11c shows that both the DAS and the RM algorithms are able to correctly locate the two targets. However, in both cases, some ghosts appear in the image with intensity comparable with that produced by the metallic post. This problem is probably due to errors caused by the non-perfect positioning of the antennas that are mounted on a manually moved trolley and by multiple reflections between the obstacles and the wall.

IV. Conclusion

The delay and sum and range migration algorithms have been compared as imaging techniques for a MIMO stepped-frequency radar system. These algorithms have been applied to analytical, simulated, and measured data both in the absence and in the presence of a wall between the antenna and the target. Both techniques were able to accurately reconstruct the position of targets behind a wall. The DAS presents a wider angle of non-ambiguity while the RM is faster. A further improvement of the DAS in terms of accuracy in the target positioning has been achieved by applying the Fermat's principle. As future development, to obtain more accurate measured data, a system based on a set of Vivaldi antennas, operating in the 1-3 GHz band, driven by a couple of single pole six throw switches (PE71S6088) will be used in the experimental setup.

References

[1] M.G. Amin, "Through the wall radar imaging", CRC Press, 2011.
[2] G. Wang, C. Gu, T. Inoue, C. Li, "A hybrid FMCW-interferometry radar for indoor precise positioning and versatile life activity monitoring, " IEEE Trans. on Microwave Theory and Techniques, vol. 62, no 11, pp. 2812-2822, 2014.
[3] G. L. Charvat, L. C. Kempel, E. J. Rothwell, C. M. Coleman, and E. L. Mokole, "A through-dielectric radar imaging system," IEEE Transactions on Antennas and Propagation, vol. 58, no 8, pp. 2594-2603, Aug. 2010
[4] J.E. Peabody, G.L. Charvat, J.Goodwin, M. Tobias, "Through-wall imaging radar", Lincoln Laboratory Journal, vol. 9, no 1, pp. 62-72, 2012
[5] F. Adib, C.Y. Hsu, H. Mao, D. Katabi, F. Durand, "Capturing the human figure through a wall" ACM Trans. Graph., vol. 34, no 6, November 2015.
[6] M. A. Ressler, L. H. Nguyen, F. J. Koenig, G. Smith, "Synchronous impulse reconstruction (SIRE) radar sensor for autonomous navigation", US Army Research Laboratory, 2006.
[7] X. P. Masbernat, M. G. Amin, F. Ahmad, C. Ioana, "An MIMO-MTI Approach for Through-the-Wall Radar Imaging Applications," Proc. 5th Int. Waveform Diversity and Design Conf., Canada, 2010, pp. 188-192.
[8] F. Ahmad, and M. G. Amin, "Wall clutter mitigation for MIMO radar configurations in urban sensing," Proc. 11th Int. Conf. on Information Science, Signal Processing and their Applications, 2012, pp. 1165-1170.
[9] M. G. Amin, and F. Ahmad, "Compressive sensing for through-the-wall radar imaging," Journal of Electronic Imaging vol. 22, no 3, pp. 1-21, Jul–Sep 2013,
[10] S. Pisa, E. Piuzzi , E. Pittella, P. D'Atanasio, A. Zambotti, G. Sacco, "Power Budget and Reconstruction Algorithms for Through the Wall Radar Imaging Systems" Proceedings of the 2018 IEEE/MTT-S International Microwave Biomedical Conference (IMBioC),15 June 2018 . Philadelphia, Pennsylvania, USA, pp. 208-210.
[11] G. A. Balanis, "Advanced engineering electromagnetics", John Wiley & Son, USA, 1989.
[12] M. Karaman, P.-C. Li, and M. O'Donnell, "Synthetic aperture imaging for small scale systems," IEEE Transactions on Ultrasonics, Ferro-electrics, and Frequency Control, vol. 42, no. 3, pp. 429–442, 1995.
[13] F. Fioranelli, S. Salous, I. Ndip, and X. Raimundo, "Through-the-wall detection with gated FMCW signals using optimized patch-like and Vivaldi antennas," IEEE Trans. On Antennas and Propagation, vol. 63, no 3, pp. 1106-1117, 2015.
[14] J. Kowalik, and M. Osborne, "Methods for Unconstrained Optimization Problems," American Elsevier, New York, New York, 1968.
[15] W.G. Carrara, R.S. Goodman, and R.M. Majewski, Spotlight Synthetic Aperture Radar Signal Processing Algorithms, Artech H., MA, 1995.
[16] G. L. Charvat, "Small and Short-Range Radar Systems" CRC Press, Boca Raton, 2014.

Stefano Pisa (M'91–SM'16) received the Electronic Engineering and Ph.D. degrees from the University of Rome "La Sapienza," Rome, Italy, in 1985 and 1988, respectively. In 1989, he joined the Department of Information Engineering, Electronics and Telecommunications (DIET), Sapienza University of Rome as a Researcher. Since 2001, he has been an Associate Professor with the same university. His research interests are the interaction between electromagnetic fields and biological systems, therapeutic and diagnostic applications of electromagnetic fields, medical applications of radar, and the modeling and design of MW circuits. He has authored over 170 scientific papers. He serves as a reviewer for various international journals. Prof. Pisa is a Senior member of the IEEE Microwave Theory and Techniques Society, and a member of the Italian Society of Electromagnetics (SIEm).

Emanuele Piuzzi (M'09) received the M.S. (cum laude) and Ph.D. degrees in electronic engineering from the Sapienza University of Rome, Rome, Italy, in 1997 and 2001, respectively. He is currently an Associate Professor with the Department of Information Engineering, Electronics and Telecommunications, Sapienza University of Rome, where he is engaged in teaching electrical measurements. He is the coauthor of over 140 publications. His current research activities include the measurement of dielectric characteristics of fluids and granular materials through time- and frequency-domain reflectometry approaches, impedance pneumography, ultrawideband radar techniques for the monitoring of cardiopulmonary activity in patients, and electrical impedance tomography. Dr. Piuzzi is a member of the IEEE Instrumentation and Measurement Society, of the Italian Group of Electrical and Electronic Measurements (GMEE), and of the Italian Electrotechnical Committee (CEI). He serves as a reviewer for different international journals.

Erika Pittella (M'17) received the M.S. (cum laude) and Ph.D. degrees in electronic engineering from the Sapienza University of Rome, Rome, Italy, in 2006 and 2011, respectively. She is currently a Research Associate with the Department of Information Engineering, Electronics and Telecommunications, Sapienza University of Rome. Her research interests are related to the measurement of complex permittivity of materials, time domain reflectometry applications and biomedical instrumentation design. Her research interests also include the modeling of ultrawideband radars for the remote monitoring of cardiorespiratory activity and the design of sources, antennas, and receivers of such systems. Dr. Pittella is an Associate Editor of IET Microwaves, Antennas, and Propagation. She is a member of the IEEE Instrumentation and Measurement Society and of the Italian Group of Electrical and Electronic Measurements (GMEE).

P. D'Atanasio was born in Rome, Italy, in 1959. He received the Full Degree (*summa cum laude*) in Physics from the Sapienza University of Rome, Rome, Italy, in 1986. He joined the Italian National Agency for New Technologies, Energy and Sustainable Economic Development, Rome, as a Researcher, in 1988. Since 2000, he is responsible of the Electromagnetic Compatibility Laboratory and since 2011 he is Director of Research having also the responsibility of the qualification tests (EMC/EMI, vibration, and seismic). His current research interests include electromagnetic measurements of radar cross section, antenna characterization, dielectric spectroscopy measurements, interaction between electromagnetic fields, and biological systems. Dr. D'Atanasio is a member of the Italian Society of Physics and the Italian Electrotechnical Committee.

A. Zambotti was born in Rome, Italy, in 1963. He received high school diploma in Industrial Electronics in 1982. He was a System Technician of electro-optical infrared systems with Selenia-Alenia Company, Pomezia, Italy, from 1985 to 1993. In 1993, he joined the Italian National Agency for New Technologies, Energy and Sustainable Economic Development (ENEA), Rome, as a Technician, where he participated in the realization and setup of the Metrological Centre with the ENEA's Trisaia Research Centre. Since 2000, he has been with the Electromagnetic Compatibility Laboratory, ENEA's Casaccia Research Centre, Rome, where he serves as the Laboratory Technician for electromagnetic compatibility/electromagnetic interference measurements and tests according to MIL and IEC standards. He also collaborates in research activities on dielectric spectroscopy measurements, antenna, and radar cross section measurements.

G. Sacco (S'18) received the B.S. (cum laude) in Clinical Engineering and the M.S. (cum laude) in Biomedical Engineering from the Sapienza University of Rome, Rome, Italy, in 2015 and 2017 respectively. She is currently working toward the Ph.D. degree in Information and Communications Technology (ICT) at Sapienza University of Rome. Her research interests are electromagnetism applied to the medicine and the modelling and design of microwave circuits and antennas. Main of her research activities are related to the modelling of radars for the remote monitoring of cardiorespiratory activity and to development of Electron Paramagnetic Resonance (EPR) systems.